

A Highly Efficient and Accurate Algorithm for Solving the Partial Differential Equation in Cardiac Tissue Models

JICHAO ZHAO¹, YINBIN JIN², LI MA³, ROBERT M. CORLESS¹

¹Department of Applied Mathematics
University of Western Ontario
London, Ontario, N6A 5B7, Canada

²School of Life Science and Technology, ³the First Hospital
Xi'an Jiaotong University
Xi'an, 710049, China

Abstract:- We give a highly efficient, accurate and unconditionally stable algorithm to solve the partial differential equation for simulating the action potential propagation through cardiac tissue. In the new algorithm, we discretize the space domain by combining a compact finite difference scheme with an alternating direction implicit (ADI) scheme, which has fourth-order accuracy for interior mesh points, and second-order accuracy for boundary mesh points. In our computer simulation, we test the new method on a two dimensional Luo-Rudy phase I action potential model. For a fixed mesh grid N , the compact finite difference ADI method yields 50% more accuracy than the Crank-Nicolson ADI method. Furthermore, it costs almost the same amount of time as the Crank-Nicolson ADI method. On the other hand, if we want to obtain the same accuracy, it only costs 49% ~ 65% of computational time if we use our compact finite difference ADI method instead of the Crank-Nicolson ADI method.

Key-Words:- Compact finite difference method, ADI, Cardiac tissue models, Computer simulation, Spiral wave

1 Introduction

Cardiac tissue conduction models and computer simulation study have made the realization of the heart from qualitative analysis to quantitative analysis. These could be invaluable in the research of the foundation of cardiac arrhythmia and in the development of drugs for the treatment of various diseases caused by cardiac electric disorders. Until now there are two major classes of models of cardiac tissue: ionic models (Luo and Rudy 1994, Noble *et al* 1998) and FitzHugh-Nagumo models (FHN) (FitzHugh 1961, Aliev and Panfilov 1996, Fenton and Karma 1998). No matter which model we use for computer simulation study, we need to solve a system of stiff, coupled ordinary differential equations (ODE's) and a partial differential equation (PDE) with non-flux boundary conditions. A lot of techniques have been developed for solving these ODE's, such as the Runge-Kutta method (Noble 1962, McAllister Beeler *et al* 1975, and Reuter 1977) and an adaptive time step method (Luo and Rudy 1991). As we know, for high dimensional problems, for example in the three dimen-

sional case, the computational time is inversely proportional to the third degree of the space step h and to the first degree of the time step Δt . In other words, the total computational efficiency depends heavily on the numerical schemes for discretizing the space. In previous work [6, 11, 13, 10, 4, 7, 12], the authors used first-order accurate methods: explicit Ruler scheme, or implicit Ruler scheme, or second-order Crank-Nicolson method to discretize the space, and then apply the alternating directional implicit (ADI) to reduce the high dimensional problem to one dimension and solve them. In this paper, we will give a compact finite difference ADI scheme, which has fourth-order accuracy for interior mesh points, and second-order accuracy for boundary mesh points, but use no more operations than the corresponding Crank-Nicolson ADI method. This scheme is unconditionally stable when combined with the first-order backward-time or second-order centered-time approximations. In our numerical experiments, we employ the compact finite difference method ADI method combined with centered-time approximations for a sim-

ple two dimensional PDE with non-flux boundary conditions, and it turns out that for a fixed mesh grid N , the compact finite difference ADI method yields 50% more accuracy than the Crank-Nicolson ADI method. Moreover it costs almost the same amount of time as the Crank-Nicolson ADI method. On the other hand, if we want to obtain the same accuracy, it saves a lot of time if we use compact finite difference ADI method instead of the Crank-Nicolson ADI method. Next we take the Luo-Rudy phase I model as an illustration to show how to use the fourth-order compact finite difference ADI scheme for two dimensional cardiac tissue conduction models. Our computer simulation confirms that the compact finite difference centered-time ADI scheme is a highly accurate, efficient and unconditionally stable method for cardiac tissue conduction models.

2 Compact Finite Difference ADI Method

We describe the algorithm using the compact finite difference method and ADI scheme for two dimensional PDE problems in this part. Suppose we want to solve the following PDE by the compact finite difference ADI scheme

$$\frac{\partial V}{\partial t} = D\left(\frac{\partial^2 V}{\partial x^2} + \frac{\partial^2 V}{\partial y^2}\right), (x, y) \in \Omega, t \in (0, T]. \quad (1)$$

Here V is a function of x , y and t , and D is a given constant. With the initial condition:

$$V|_{t=0} = \varphi_0(x, y), \quad (2)$$

and non-flux boundary conditions

$$\frac{\partial V}{\partial x}\Big|_{x=x_{min}, x=x_{max}} = \frac{\partial V}{\partial y}\Big|_{y=y_{min}, y=y_{max}} = 0. \quad (3)$$

For simplicity, we consider the case that domain $\Omega = [0, d; 0, d]$ is a square. First discretize the domain Ω by

$$x_i = ih, y_j = jh, 0 \leq i, j \leq N, h = \frac{d}{N},$$

and the temporal space

$$t_k = k\Delta t, k = 0, 1, \dots, M, \Delta t = \frac{T}{M}.$$

To discretize the PDE (1) along the x-axis, we can use the second-order central difference scheme:

$$\frac{\partial^2 V_{i,j,t}}{\partial x^2} = \frac{V_{i-1,j,t} - 2V_{i,j,t} + V_{i+1,j,t}}{h^2}, \quad (4)$$

here $V_{i,j,t} = V(x_i, y_j, t)$ and $i = 1, 2, \dots, N - 1$. For boundary points, we use the following first-order schemes

$$\frac{\partial^2 V_{0,j,t}}{\partial x^2} = \frac{-2V_{0,j,t} + 2V_{1,j,t}}{h^2} - \frac{2}{h} \frac{\partial V_{0,j,t}}{\partial x}, \quad (5)$$

and

$$\frac{\partial^2 V_{N,j,t}}{\partial x^2} = \frac{-2V_{N,j,t} + 2V_{N-1,j,t}}{h^2} + \frac{2}{h} \frac{\partial V_{N,j,t}}{\partial x}. \quad (6)$$

While in this paper we develop a compact finite difference scheme to solve (1) with non-flux boundary conditions (3). For the interior points $i = 1, 2, \dots, N - 1$, we use the following fourth-order accurate formula

$$\begin{aligned} \frac{\partial^2 V_{i-1,j,t}}{\partial x^2} + 10 \frac{\partial^2 V_{i,j,t}}{\partial x^2} + \frac{\partial^2 V_{i+1,j,t}}{\partial x^2} \\ = \frac{12V_{i-1,j,t} - 24V_{i,j,t} + 12V_{i+1,j,t}}{h^2}. \end{aligned} \quad (7)$$

This formula and all the following compact finite difference formulae can be obtained by the Taylor expansion, refer to [2, 8] for details. For the mesh grid point $i = 0$, we use the following second-order difference formula

$$\begin{aligned} \frac{\partial^2 V_{0,j,t}}{\partial x^2} + \frac{1}{2} \frac{\partial^2 V_{1,j,t}}{\partial x^2} \\ = \frac{-3V_{0,j,t} + 3V_{1,j,t}}{h^2} - \frac{3}{h} \frac{\partial V_{0,j,t}}{\partial x}, \end{aligned} \quad (8)$$

for taking the advantages that we already have known the non-flux boundary value of $\frac{\partial V_{0,j,t}}{\partial x}$. For the same reason, we deal with non-flux boundary condition by the following difference approximations when the mesh grid point $i = N$

$$\begin{aligned} \frac{\partial^2 V_{N,j,t}}{\partial x^2} + \frac{1}{2} \frac{\partial^2 V_{N-1,j,t}}{\partial x^2} \\ = \frac{-3V_{N,j,t} + 3V_{N-1,j,t}}{h^2} + \frac{3}{h} \frac{\partial V_{N,j,t}}{\partial x}. \end{aligned} \quad (9)$$

To make life easier, let δ_x denote the linear difference operator for the right side of (7), (8), and (9), i.e.,

$$\delta_x V_{i,j,t} = \begin{cases} \frac{(-3V_{0,j,t} + 3V_{1,j,t})}{h^2}, & i = 0, \\ \frac{(-3V_{N,j,t} + 3V_{N-1,j,t})}{h^2}, & i = N, \\ \frac{12V_{i-1,j,t} - 24V_{i,j,t} + 12V_{i+1,j,t}}{h^2} & \text{others.} \end{cases}$$

Note in the above definition of operator δ_x , we already use non-flux conditions (3) to simplify the expression.

Let L_x denotes the linear operator for the left side of (7), (8), and (9), namely

$$L_x V_{i,j,t} = \begin{cases} -3V_{0,j,t} + \frac{1}{2}V_{1,j,t}, & i = 0 \\ V_{N,j,t} + \frac{1}{2}V_{N-1,j,t}, & i = N \\ 12(V_{i-1,j,t} - 2V_{i,j,t} + V_{i+1,j,t}), & \text{others.} \end{cases}$$

Then we can write (7), (8), and (9) into the following symbolical uniform

$$L_x \frac{\partial^2 V_{i,j,t}}{\partial x^2} = \delta_x V_{i,j,t}, \quad i = 0, 1, \dots, N. \quad (10)$$

By using the same way to deal with the variable y , we obtain

$$L_y \frac{\partial^2 V_{i,j,t}}{\partial y^2} = \delta_y V_{i,j,t}, \quad j = 0, 1, \dots, N. \quad (11)$$

The meanings for operators δ_y and L_y are obvious. Applying the two formulae (10) and (11) on (1), we obtain

$$\frac{\partial V(x, y, t)}{\partial t} = D \left(\frac{\delta_x V_{i,j,t}}{L_x} + \frac{\delta_y V_{i,j,t}}{L_y} \right), \quad (12)$$

or

$$L_y L_x \frac{\partial V(x, y, t)}{\partial t} = D(L_y \delta_x + L_x \delta_y) V_{i,j,t}. \quad (13)$$

For the equation (13), we may use the first-order explicit forward-time scheme or implicit backward-time scheme to approximate the partial derivative $\frac{\partial V}{\partial t}$ in (13). Here we employ the second-order centered-time approximation and show how to solve it by the ADI scheme. Adding the term $\frac{\Delta t^2 D^2}{4} \delta_x \delta_y (V_{i,j}^{k+1} - V_{i,j}^k)$ to the left side of equation (13) after we discretize the time space, then we rearrange it into the following form:

$$\begin{aligned} & (L_y - \frac{\Delta t D}{2} \delta_y) (L_x - \frac{\Delta t D}{2} \delta_x) V_{i,j}^{k+1} \\ &= (L_y + \frac{\Delta t D}{2} \delta_y) (L_x + \frac{\Delta t D}{2} \delta_x) V_{i,j}^k, \end{aligned} \quad (14)$$

here $V_{i,j}^k$ stands for $V(x_i, y_j, t_k)$. To solve (14) efficiently and accurately, we introduce an intermediate variable V^* , and apply the ADI-like scheme [9] or the so called approximate-factorization-implicit (AFI) method [3], yielding

$$\begin{aligned} & (L_y - \frac{\Delta t D}{2} \delta_y) V_{i,j}^* \\ &= (L_y + \frac{\Delta t D}{2} \delta_y) (L_x + \frac{\Delta t D}{2} \delta_x) V_{i,j}^k, \end{aligned} \quad (15)$$

$$(L_x - \frac{\Delta t D}{2} \delta_x) V_{i,j}^{k+1} = V_{i,j}^*, \quad (16)$$

where $0 \leq i, j \leq N$, and $0 \leq k \leq M - 1$. By using the definitions for the operators δ_x , δ_y , L_x , and L_y in equation (7), (8) and (9), we rewrite the coefficients of the left side of equations (15) and (16) into a same matrix form and the nonzero elements are given by

$$A = \begin{bmatrix} 1 + \frac{3}{2}\lambda & \frac{1}{2} - \frac{3}{2}\lambda & & & \\ 1 - 6\lambda & 10 + 12\lambda & 1 - 6\lambda & & \\ & \ddots & \ddots & \ddots & \\ & & 1 - 6\lambda & 10 + 12\lambda & 1 - 6\lambda \\ & & & \frac{1}{2} - \frac{3}{2}\lambda & 1 + \frac{3}{2}\lambda \end{bmatrix},$$

here $\lambda = \frac{D \Delta t}{h^2}$. If we assume the values of V^k are known, we can easily compute the values for V^* by the formula (15) and then compute for V^{k+1} by the formula (16) taking the advantages that A is a tri-diagonal matrix. One thing we must point out is that we don't know the non-flux boundary values $\frac{\partial V^*}{\partial y} |_{y=y_{min}}$ and $\frac{\partial V^*}{\partial y} |_{y=y_{max}}$ when we use the formula (15). There are a lot of ways to deal with this problem, the simplest way is just to impose an additional condition $\frac{\partial V^*}{\partial y} |_{y=y_{min}} = \frac{\partial V^*}{\partial y} |_{y=y_{max}} = 0$.

The compact finite difference ADI scheme has the fourth-order accuracy for interior points and second order accuracy for boundary points. If it is combined with the first-order backward-time or second-order centered time approximations for the PDE (1), the implicit scheme is unconditionally stable.

2.1 Numerical Experiments

To show the accurate order of our compact finite difference ADI schemes, we first test a simple two dimensional example: choose parameters $D = 1, \Omega = [0, 1; 0, 1]$ in the PDE (1), and give the initial condition by

$$\varphi_0(x, y) = 10 \cos(\pi x) \cos(\pi y). \quad (17)$$

For this example, we easily know the exact solution is

$$V(x, y, t) = 10e^{-2\pi^2 t} \cos(\pi x) \cos(\pi y). \quad (18)$$

Let $T = 0.01$, and the fixed temporal step $\Delta t = 10^{-5}$. The maximum absolute error is defined as the maximum value of the absolute difference between the exact solutions and approximation solutions at all partition points. We compare the maximum absolute errors and computational times obtained by the compact finite difference ADI method with those obtained by the Crank-Nicolson ADI method when we vary the mesh grid N in Fig. 1. From the Fig. 1 (a), we can see that

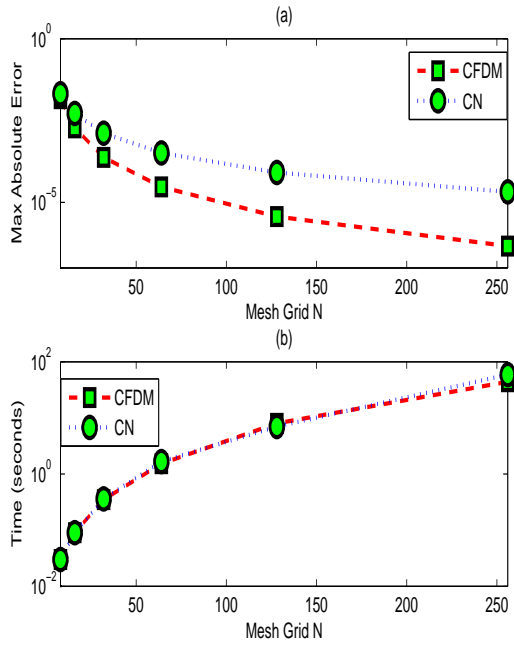


Figure 1: Comparing max absolute errors and times.

the compact finite difference ADI method can achieve higher accuracy than the Crank-Nicolson ADI method. By using the following formula to estimate the accurate order p of different methods

$$p = \log_2\left(\frac{e_h}{e_{h/2}}\right), \quad (19)$$

here e_h denotes the maximum absolute error with the spacial step h . We know that the compact finite difference ADI method can obtain $O(h^3)$ of accuracy for the whole space domain, while the Crank-Nicolson ADI method is $O(h^2)$. It means that for the fixed grid mesh N , the compact finite difference ADI method yields 50% of accuracy more than Crank-Nicolson ADI method; furthermore we spend no more operations by using the compact finite difference ADI method than using the Crank-Nicolson ADI method for a fixed grid mesh N by Fig. 1 (b). From the other hand, say we want to obtain the same accuracy, it saves a lot of time if we use the compact finite difference ADI method. For example, to obtain the maximum absolute error $O(10^{-5})$, the Crank-Nicolson ADI method needs about 59 seconds with the mesh grid $N = 256$, while the compact finite difference ADI method takes only 2 seconds with the mesh grid $N = 64$.

3 Solving Cardiac Tissue Conduction Models

It is well known that there are two major classes of models of cardiac tissue: ionic models and FHN models. The output data from computer simulation can be used for further study on isopotential contour lines, spiral wave tip trajectories, and pseudo-electrocardiogram. No matter which model we use for computer simulation study, we need to solve a system of stiff, coupled ODE's and a PDE with non-flux boundary conditions. In this section, we take Luo-Rudy phase I model as a demonstration to show how to use the the compact finite difference ADI scheme for the two dimensional cardiac tissue conduction models. It is quite straightforward to extend the new scheme for FHN model. In our computer simulation, we imitate spiral waves produced by the output of the compact finite difference ADI scheme and compare them with those generated by the Crank-Nicolson ADI scheme. The experiments confirm that the compact finite difference centered-time ADI scheme is a highly accurate, efficient and unconditionally stable method for cardiac tissue conduction models.

3.1 Algorithm

The PDE for cardiac conduction in homogeneous tissue is described by the following reaction-diffusion-like equation [12, 13]:

$$\frac{\partial V}{\partial t} = -\frac{I_{ion}}{C} + D\left(\frac{\partial^2 V}{\partial x^2} + \frac{\partial^2 V}{\partial y^2}\right). \quad (20)$$

Where D is the diffusion coefficient related to gap junctions between cells, C is membrane capacitance, V is local membrane potential, and I_{ion} is the total ionic current density. Non-flux boundary conditions are used for two dimensional tissue model simulations. I_{ion} is a function of voltage V , gating variables Y_1, Y_2, \dots, Y_p , and ion concentrations Z_1, Z_2, \dots, Z_q . The gating variables Y_i hold the following system of ODE's

$$\frac{\partial Y_i(t)}{\partial t} = \alpha_i(1 - Y_i(t)) - \beta_i Y_i(t). \quad (21)$$

Where α_i and β_i are rate constants and are voltage-dependent functions. The ion concentrations Z_i satisfy the following set of ODE's

$$\frac{\partial Z_i(t)}{\partial t} = f_i(I_{Z_i}, V, Z_i), \quad (22)$$

here I_{Z_i} is the Z_i related ionic current.

The operator splitting method and compact finite difference ADI method are used for the PDE (20), the gating variables (21) are integrated by the algorithm of Rush and Larsen [10], and adaptive time step methods are used to integrate (22). The algorithm has three steps:

Step I: Take the results at time t as the initial condition and apply the compact finite difference ADI method to solve the following PDE

$$\frac{\partial V}{\partial t} = D\left(\frac{\partial^2 V}{\partial x^2} + \frac{\partial^2 V}{\partial y^2}\right), \quad (23)$$

with a temporal step length $\frac{\Delta t}{2}$.

Step II: Use the results of step I as the initial condition to integrate the following ODEs

$$\frac{\partial V}{\partial t} = -\frac{I_{ion}}{C}, \quad (24)$$

$$\frac{\partial Y_i(t)}{\partial t} = \alpha_i(1 - Y_i(t)) - \beta_i Y_i(t), \quad i = 1, \dots, p, \quad (25)$$

$$\frac{\partial Z_i(t)}{\partial t} = f_i(I_{Z_i}, V, Z_i), \quad i = 1, 2, \dots, q, \quad (26)$$

with a temporal step length Δt .

Step III: Set the results of step II as the initial condition and solve the following PDE with a temporal step length $\frac{\Delta t}{2}$ again by the compact finite difference ADI method

$$\frac{\partial V}{\partial t} = D\left(\frac{\partial^2 V}{\partial x^2} + \frac{\partial^2 V}{\partial y^2}\right). \quad (27)$$

3.2 Computer Simulation

Let's implement the above algorithm for cardiac tissue conduction of the two dimensional case. In our simulation, we choose $C = 1\mu\text{F}/\text{cm}^2$, $D = 0.001\text{cm}^2/\text{ms}$, cardiac tissue sheet Ω is $6\text{cm} \times 6\text{cm}$, and $T = 500\text{ms}$.

Fig. 2 (A), (B), (C), and (D) are the imitated spiral waves produced by the output of the Crank-Nicolson ADI scheme with the fixed $T = 500$ and varied spacial step h ; Fig. 2 (E), (F), (G), and (H) are the imitated spiral waves produced by the compact finite difference ADI scheme. It is easy to see there are notable changes in the imitated spiral waves by the Crank-Nicolson ADI scheme with increasing the spacial step h , while they are quite smaller by the compact finite difference ADI scheme. That is a sign that the new method is more accurate.

Table 1 and Table 2 list computational times and conduction velocity by the Crank-Nicolson ADI scheme and compact finite difference ADI scheme respectively

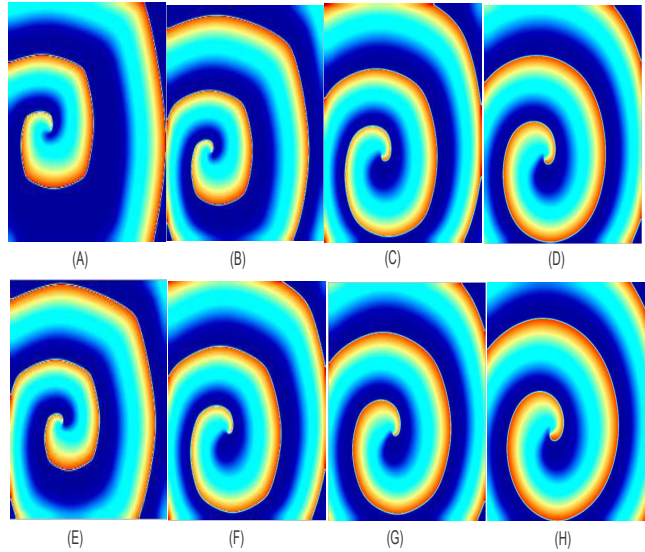


Figure 2: Spiral waves (A), (B), (C) and (D) generated by the output of the Crank-Nicolson ADI scheme and (E), (F), (G), and (H) by the compact finite difference ADI scheme with the fixed $T = 500$ and varied spacial step h . And the spacial step h is 0.030cm , 0.025cm , 0.020cm , and 0.015cm respectively. The pattern of (A) has a considerable deviation from that of the others.

with the fixed $T = 500$ and varied spacial step h . There is an another rule to judge which method is more accurate: the less the conduction velocity changes, the more accurate is the method. From this point, the compact finite difference ADI scheme as well prevails against the Crank-Nicolson ADI scheme. When we look at the computational times, it takes a little longer time for the compact finite difference ADI scheme than the Crank-Nicolson ADI scheme at a fixed spacial step h . The reason is that the conduction speed of the action potential obtained by the Crank-Nicolson ADI scheme is lower than the one obtained by the compact finite difference ADI scheme. The repolarized area, as well as the area at reset potential, is larger with lower conduction speed. When we use adaptive time step methods to solve ODE's, it takes shorter time to solve them. If we want to obtain the same order of accuracy, the compact finite difference ADI scheme saves much more times. By looking at the shape of imitated spiral waves in Fig.2, we believe (B) and (E), (C) and (F), (D) and (G) to be the same level of accuracy. It means that the compact finite difference ADI scheme only needs 65%, 64%, and 49% of computational times used by the Crank-Nicolson ADI scheme according to the computational times in Table 1 and Table 2.

Table 1: Computational times and conduction velocity by the Crank-Nicolson ADI method with the fixed $T = 500$ and varied spacial step h :

| Step length h | Computational time | Conduction velocity |
|-----------------|--------------------|---------------------|
| 0.015cm | 6125s | 37.5cm/s |
| 0.020cm | 2943s | 34.1cm/s |
| 0.025cm | 1867s | 31.3cm/s |
| 0.030cm | 1126s | 27.9cm/s |

Table 2: Computational times and conduction velocity by the compact finite difference ADI method with the fixed $T = 500$ and varied spacial step h :

| Step length h | Computational time | Conduction velocity |
|-----------------|--------------------|---------------------|
| 0.015cm | 6140s | 40.0cm/s |
| 0.020cm | 3010s | 37.6cm/s |
| 0.025cm | 1897s | 35.9cm/s |
| 0.030cm | 1212s | 32.0cm/s |

4 Conclusions

We give a highly efficient, accurate and unconditionally stable compact finite difference ADI scheme for solving the partial differential equation in cardiac tissue models of the two dimensional case. And we are now working on extending our work to the three dimensional case, and we expect to save more time since the computational time is inversely proportional to the third degree of the space step.

References

- [1] C. H. Luo, and Y. Rudy, "A dynamical model of the cardiac ventricular action potential: I. Simulations of ionic currents and concentration changes". *Circ Res*, vol. 74, pp. 1071-1096, 1994.
- [2] J. Zhao, R.M. Corless, and M. Davison, "Financial applications of symbolically generated compact finite difference formulae", *International workshop on symbolic-numerical computation Proceedings*, Xi'an, China, pp. 220-234, 2005.
- [3] J. D. Hoffman, "Numerical methods for engineers and scientists", Marcel Dekker, Inc., New York, 2001.
- [4] J. A. Trangenstein, K. Skouibine and W. K. Allard, "Operator splitting and adaptive method refinement for the Fitzhugh-Nagumo problem", submitted to *SIAM Journal on Scientific Computing*, 2000.
- [5] N. A. Wedge, M. S. Branicky, and M. C. ÇavuŞođlu, "Computationally efficient cardiac bioelectricity models toward whole-heart simulation", *Proceedings of the 26th Annual International Conference of the IEEE EMBS*, San Francisco, CA, September 1-5, 2004.
- [6] O. Bernus, H. Verschelde and A. V Panfilov, "Modified ionic models of cardiac tissue for efficient large scale computations", *Phys. Med. Biol.* 47, pp. 1947-1959, 2002.
- [7] R. M. Shaw and Y. Rudy, "Ionic mechanisms of propagation in cardiac tissue", *Circulation Research*, Vol. 81, pp. 727-741, 1997.
- [8] R.M. Corless, J. Rokicki and J. Zhao, FINDIF, a routine for generation of finite difference formulae, Share Library package 1994, and upgraded to n dimensions for "iguana".
- [9] S. Karaa, and J. Zhang, "High order ADI method for solving Unsteady convection-diffusion problems", *Technical Report No. 375-03*, University of Kentucky, 2003.
- [10] S. Rush, and H. Larsen, "A practical algorithm for solving dynamic membrane equations", *IEEE Trans. Biomed. Eng.*, vol. BME-25, pp. 389-392, 1979.
- [11] W. Quan, S. J. Evans and H. M. Hastings, "Efficient Integration of a realistic two-dimensional cardiac tissue model by domain decomposition", *IEEE Transactions on Biomedical Engineering*, Vol. 45(3), 1998.
- [12] Y. B. Jin, L. Yang, H. Zhang, Y. H. Kuo, Y. C. Huang, and D. Z. Jiang, "Numerical algorithm for conduction of action potential in two-dimensional cardiac ventricle tissue", *Journal of Xi'an Jiaotong University*, Vol. 38(8), pp. 851-854, 2004.
- [13] Z. L. Qu, and Alan Garfinkel, "An Advanced algorithm for solving partial differential equation in cardiac conduction", *IEEE Trans. Biomed. Eng.*, vol. BME-46, pp. 1166-1168, 1999.